A_2 of Fig. 1) normalizing for the same number of particles. In this way an accurate correction factor for beta intensity observed at any particular energy was deduced. This factor was then applied to the experimental data for C^{14} (curve B_1 of Fig. 1), and in Fig. 3 we show separately a plot of this corrected data. The full curve in Fig. 3 represents the theoretical form of the C^{14} spectrum, if the decay is allowed. It is seen to fit excellently the adjusted experimental values and the agreement from less than 3 kev upwards constitutes strong evidence that the carbon spectrum is allowed in form.

One of us (A.M.) would like to express his thanks to Professor P. I. Dee, F. R. S. for his generous hospitality throughout his stay in Glasgow. He is indebted to Professor A. Peterlin, Institute of Physics, Ljubljana, for a prolonged leave of absence and the grant of a scholarship.

PHYSICAL REVIEW VOLUME 96, NUMBER 2 OCTOBER 15, 1954

Total Cross Sections of 208-Mev and 315-Mev Protons for Light Elements*

HERVASIO G. DE CARVALHO†
Institute for Nuclear Studies, The University of Chicago, Chicago, Illinois
(Received June 25, 1954)

Transmission measurements were performed with an external collimated proton beam of The University of Chicago 170-inch synchrocyclotron. Total cross sections of the neutron and ten light elements (H and D, Li, B, Be, C, N, O, Al, S, and Cl) were measured by coincidence and anticoincidence methods at proton energies of 208 and 315 Mev at several subtended angles.

The cross sections obtained include all processes except the Coulomb scattering, for which corrections were applied. The corrected cross sections, measured at different subtended angles ("poor geometries") were plotted with their statistical uncertainties as a function of the solid angle subtended or of the angle, and extrapolated to zero degrees ("good geometry").

Only a limited number of previous investigations of the light elements at high particle energies have been made. The results found in the present study for the proton total cross sections for the various elements were comparable to the available published neutron total cross sections measured at the same energies.

It was found, by application of the transparent optical model, that cross sections measured were consistent with a nuclear radius $R=1.23A^{\frac{1}{3}}\times10^{-13}$ cm and an absorption coefficient $K=0.5\times10^{13}$ cm^{-1}.

I. INTRODUCTION

THE measurement of the total cross section of nuclei for high-energy nucleons gives information about the nuclear radius and the behavior of the high-energy nucleons within nuclear matter. In particular it gives information about the Serber[1] transparency effect of nuclear matter to high-energy nucleons which up to the present time has been studied mainly with neutrons.

In the past most of the total cross-section measurements were carried out using neutrons because of the difficulties involved in experiments with protons. The main results of this work with neutrons are well summarized in a recent paper by Nedzel.[2]

In principle, the measurement of total cross sections for neutrons does not present a complex problem. Neutrons have no charge and consequently their electromagnetic interactions are extremely weak. Therefore, nuclear forces cause by far the most important interaction between high-energy neutrons and nuclei. The measurements of neutron total cross sections are not complicated by the large contribution of the nuclear Coulomb field, which in the case of proton scattering is responsible for a fast rise of cross section at small angles.

In general one expects that the cross section depends on the energy. Since as a rule high-energy neutrons are not monoenergetic it is useful to calculate an effective neutron energy $\bar{E}_{\text{eff}}$. This is an involved problem, which is a serious handicap for the interpretation of the measurements. A second disadvantage follows from the fact that high-energy neutrons are detected indirectly by nuclear reactions or by recoil protons produced in neutron-proton scattering.

In contrast to the neutron situation, collimated monoenergetic beams of protons are readily obtained at high energies. Owing to energy loss by ionization, however, protons of several-hundred Mev energy are not able to cross even one entire nuclear interaction mean free path. In order to measure the nuclear interaction at a given energy it consequently becomes necessary to use relatively thin absorbers. As another difficulty, Coulomb scattering does not allow the direct "good geometry" measurements of total nuclear cross sections, but these can be obtained indirectly by a

* Research supported by a joint program of the U. S. Office of Naval Research and the U. S. Atomic Energy Commission.
† On leave of absence from the Conselho Nacional de Pesquisas of Brazil.
[1] R. Serber, Phys. Rev. 72, 1114 (1947).
[2] V. A. Nedzel, Phys. Rev. 94, 175 (1954).

precise extrapolation of measurements at different "poor geometries" to the condition of "good geometry."

The research already done in this field with high-energy protons is covered by only a few papers.

Proton absorption cross sections have been measured for Be, C, Al, Cu, Pb, and U by Kirschbaum[3] for protons of average energies of 305, 240, and 185 Mev. More recently Birnbaum, Crandall, Schecter, and Millburn[4] measured the absorption cross section of a few representative elements for high-energy protons, deuterons, He^3 particles, and alpha particles by using an attenuation technique. At Brookhaven, working with 870-Mev protons, Chen *et al.*[5] are measuring absorption cross sections for Be, C, Al, Cu, Sn, and Pb.

The only measurements of total cross sections for high-energy protons are the ones published by Marshall, Marshall, and Nedzel[6] at 410 Mev and of Chen[5] at 870 Mev. Consequently, following a suggestion of Professor John Marshall, it was decided that this study would be devoted to measuring total cross sections for protons on selected elements at energies between 200 and 400 Mev.

II. GENERAL FEATURES OF THE EXPERIMENT

For reasons mainly related to the Coulomb scattering, the elements of low atomic number were chosen for investigation. Hydrogen and deuterium have a very special importance since *p-p* and *n-p* scattering cross-section data are essential for the study of the nature of nuclear forces, and for this reason careful experiments to obtain their cross sections were carried out.

The elements for which high-energy proton scattering was studied were hydrogen and deuterium, lithium, beryllium, boron, carbon, nitrogen, oxygen, aluminum, sulfur, and chlorine.

A. Nature of the Samples

The cross section of hydrogen for 315-Mev protons was measured directly by using liquid hydrogen; the cross section for 208-Mev protons was obtained from the difference of the measured cross sections of carbon and polyethylene. The proton-neutron cross section for hydrogen was obtained from the difference between the measured cross sections of equal thicknesses of heavy and light water. The oxygen, sulfur, and chlorine cross sections were obtained from the differences, respectively, between those of water and hydrogen, carbon disulfide and carbon, and carbon tetrachloride and carbon. The nitrogen cross section was measured in liquid nitrogen, by using a special Styrofoam container. For the remaining elements, solid samples were used, with the best available purity. The lithium absorber was specially prepared as follows: Li metal was cleaned under kerosene, pressed in an aluminum die under 50 atmospheres, and sealed into an aluminum can with windows 0.003 inch thick. When not in use, the sample was kept under kerosene to prevent oxidation. The boron sample was very finely powdered amorphous boron in a thin-walled Lucite cylinder.

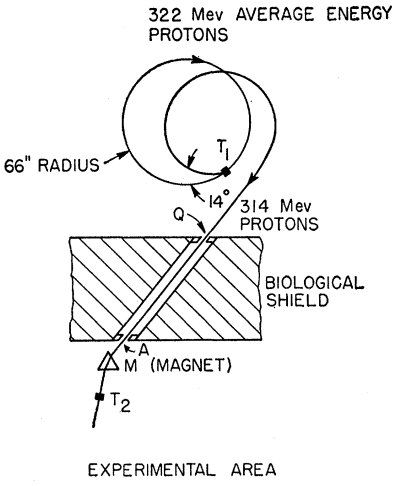

FIG. 1. Method used to select proton energy and to collimate proton beam.

B. Experimental Layout

An external well-collimated monoenergetic beam of protons was scattered out of the Chicago 170-inch synchrocyclotron from an internal beryllium target at 66 inches radius. The scattered protons were analyzed energy-wise by deflection in the fringing field of the cyclotron magnet, and then were defined as a beam by passing through two collimators in the heavy shield, (Fig. 1). The first collimator *Q*, located inside of the synchrocyclotron room, was a $\frac{1}{8}$-inch vertical slit obtained with stainless steel bricks. Outside of the biological shield was a second collimator *A* of $\frac{3}{8}$-inch diameter brass tube inside a lead brick. Following this the beam was deflected a second time with an auxiliary magnet *B*.

The arrangement of the experiment is shown in Fig. 2. The proton beam already analyzed in the fringing magnet field of the cyclotron enters the experi-

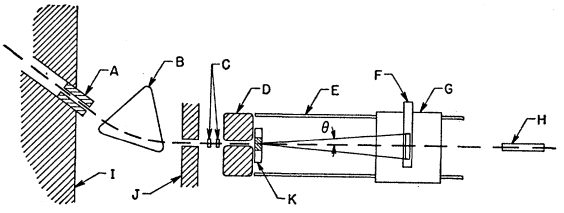

FIG. 2. Schematic arrangement of experimental apparatus (not to scale). *A*-collimator, *B*-auxiliary magnet, *C*-monitor telescope coincidence counters, *D*-shield, *E*-rails, *F*-anticoincidence counter, *G*-rolling table, *H*-cathetometer, *I*-heavy shield, *J*-auxiliary shield, *K*-target holder.

[3] A. J. Kirschbaum, thesis, University of California Radiation Laboratory Report UCRL-1967, 1952 (unpublished).
[4] Millburn, Birnbaum, Crandall, and Schecter, Phys. Rev. **95**, 1268 (1954).
[5] Chen, Leavitt, and Shapiro, Phys. Rev. **94**, 784 (1954).
[6] Marshall, Marshall, and Nedzel, Phys. Rev. **91**, 767 (1953).

mental area by the collimator A, is re-analyzed by the auxiliary magnet B, then passes through an auxiliary shield J used to avoid extraneous background.

The proton beam is defined by 2 monitoring telescope coincidence counters C, which also count the number of protons in the incoming beam in a particular measurement. The beam traversing counters C then proceeds through a heavy steel shield D and reaches the experimental sample, mounted in special target holder K.

The protons scattered out of the subtended cone of half angle θ are counted by a large anticoincidence counter F which stands on a rolling table G, movable on two strong steel rails E. As seen in Fig. 2, the anticoincidence counter F subtends cones of different half angles θ as its distance from the sample is varied. The preliminary alignment of the system was aided by a cathetometer H in the beam path farthest from the cyclotron in the end of the experimental area.

C. The Principle of Measurement

The thin sample inserted in the proton beam attenuates it exponentially. The cross section corresponding to a particular subtended angle θ is given by

$$\sigma = (1/N) \log_e(I_0/I), \quad (1)$$

where N is the number of nuclei per cm^2 in the sample, I_0 is the beam intensity at the detector counter with no sample, or for a particular measurement is the number of protons inside the subtended angle θ. I_0 is given by: $(M-B_0)$, where M is the monitoring count and B_0 is the flux of protons removed from the chosen angle. Protons passing through the telescope monitoring coincidence counters undergo both nuclear and Coulomb scattering along the path which disturbs somewhat the beam collimation. A number of protons B_0 are therefore scattered out of the subtended cone angle. I is obtained by measuring by anticoincidence the total number of protons B removed from the beam with the experimental sample in position, *viz.*: $M-B$. Therefore the cross section is given by

$$\sigma = (1/N) \log_e[(M-B_0)/(M-B)]. \quad (2)$$

D. Energy and Homogeneity of the Proton Beam

The energy of the highly collimated beam was measured from copper range measurements by using Aron's[7] range energy tables. With counters C (1, 2) in coincidence and counters 1, 2 and F (3) combined in triple coincidence, the ratio of triples *vs* doubles for different copper absorber thicknesses was taken.

By assuming that the observed experimental straggling values in copper by Mather and Segrè,[8] and by Bloembergen and Van Heerden,[9] correspond to perfect monochromatic proton beams, and using the straggling measured from the number-distance range curves in this experiment, an energy inhomogeneity of about 4 Mev for the 208-Mev proton beam and 8 Mev for the 315-Mev proton beam was obtained.

III. APPARATUS

A. Counting Rate

Since the precision of results depends on the statistical uncertainty and on the reliability of the counting system, careful attention was directed toward obtaining strict linearity and maximum stability in the counting apparatus, and at the same time minimum sensitivity to any extraneous radiation.

The arrangement of counters is shown in Fig. 2.

The protons produced by the synchrocyclotron are produced in bursts of short duration, and the counting circuits must detect, resolve, and count all protons in the beam used in the experiment.

For a cyclotron pulse length of 150 microseconds and repetition rate of 60 cycles, in order to avoid losses greater than 1 percent in the monitoring system, the resolving time of the scaling system to determine coincidences between different counters must be no less than about 10^{-7} second for a rate of about 1000 counts per second in counters 1 and 2. Losses have been tested experimentally by running the same measurement at different counting rates. At the rate of a few thousand protons per second, the cross-section measurements were only slightly higher and it was found that for counting rates of less than 600 protons the results were constant within the statistical uncertainty. Three hundred counts per second, therefore, was chosen as a safe counting rate. In this condition, the counting losses had no appreciable effect on the cross-section measurements.

B. Counters

When protons pass through the beam-monitoring counters 1 and 2 of the telescope arrangement, as stated earlier, the collimation of the beam is somewhat disturbed by Coulomb and nuclear scattering produced by the nuclei of the materials in the counters, the result being that about 1 percent of the total protons are scattered out of the beam. It happens, also, that some protons are backscattered or absorbed by the thick walls of the anticoincidence counter; furthermore, some protons are scattered by the air between the monitors and the detector. This scattered loss of beam together with accidental counts caused by stray radiation in the experimental area constitutes B_0, the anticoincidence background of our measurements. The ratio I_0/I is obtained by taking into account this background. If B_0 is the total number of protons removed from the beam without the absorber and recorded by counter F by the anticoincidence method, I_0 is obtained by subtraction of the background B_0

[7] Aron, Hoffman, and Williams, AECU-663, University of California Radiation Laboratory Report UCRL-12, 1949 (unpublished).

[8] R. L. Mather and E. Segrè, Phys. Rev. 84, 191 (1951).

[9] N. Bloembergen and J. Van Heerden, Phys. Rev. 83, 561 (1951).

from the monitoring counting rate M, *viz.*: $I_0=M-B_0$. In order to obtain I_0 close to M it is necessary to minimize B_0. This is in part obtained by reducing the thickness of the scintillation counter required for sufficient pulse size.

The monitoring counters were circular counters made of plastic scintillator "Pilot B" with $\frac{1}{8}$-inch thickness and 1-inch diameter. This thickness appeared to be very satisfactory. The anticoincidence counter F is a large circular liquid scintillator ($9\frac{1}{4}$-inch diameter by 1 inch thick) made of a solution of 3 g/liter of terphenyl in phenylcyclohexane with 10 mg/liter of diphenylhexatriene in a Lucite cell enclosed in a light-tight aluminum box. The light produced in the scintillating material by energy loss of the proton going through it is conducted by a tapered Lucite light pipe to two photomultiplier tubes in parallel which convert the scintillation into an electric pulse.

C. Electronics

The adjustment of the electronic circuits will be described later and only the general description of the equipment used will be given here. Fast counting systems and fast resolving time coincidence circuits are necessary in order to obtain reliability with the counting rate used and in order to minimize background caused by accidental coincidence.

The negative pulse coming from the anode of the photomultiplier tube, Fig. 3, with a space charge limiter circuit developed by J. Fischer, is transmitted by a condenser to a coaxial cable, of 180-Ω characteristic impedance, and to a fast distributed amplifier. The coaxial cables, in order to prevent reflections of the signal, were each properly terminated at least on one end.

In order to correct for the time of flight of the particles, and transit time of signals in the tubes, amplifiers and connecting cables, the signal was transmitted through an adjustable cable delay with a 180-Ω impedance line switch box, capable of giving integral time delays from 1 to 63 millimicroseconds. The signal pulses from the monitor counters were each amplified through two and a half distributed amplifiers of 200-megacycles band width and voltage gain of 10 each. The pulses were clipped to 8×10^{-9} second by shorted cables of proper length and fed into a two-channel crystal diode coincidence circuit developed at the University of Chicago by J. Fischer. The output of the coincidence circuit was connected to a calibrated wide-band attenuator box and fed to a Hewlett-Packard 10 megacycle (scale of one hundred) scaler through two distributed amplifiers.

The anticoincidence pulse, from the two photomultiplier tubes of the anticoincidence counter was amplified by three distributed amplifiers and connected without clipping to a diode coincidence-anticoincidence circuit which also received the pulses from the first two counters by parallel connection to the first coincidence circuit. The output of the coincidence-anticoincidence was fed to a Hewlett-Packard 10 megacycle scaler. Both fast scalers were followed by slower scalers (scale of one thousand) and a mechanical register.

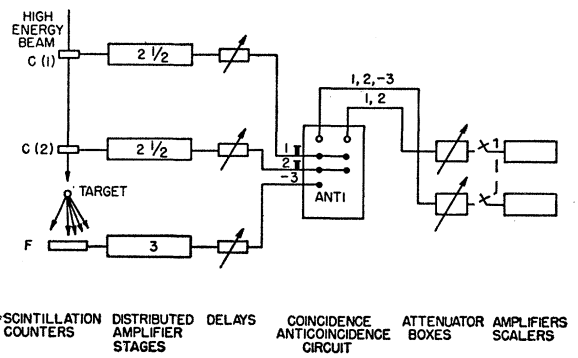

FIG. 3. Schematic illustration of the counting system, showing the anticoincidence counter arrangement and the block-diagram of the electronic system.

IV. PROCEDURE

The precision of the measurement depends on: (a) the geometrical alignment of the apparatus, (b) proper operation of the electronic equipment, (c) the correction for the effect of Coulomb scattering, and (d) the determination of the magnitude of errors inherent in the procedure chosen.

A. Geometrical Alignment

The geometrical alignment of the apparatus began with the proper location of the narrow collimating slit in the fringing magnetic field of the synchrocyclotron for a particular position of the internal beryllium target which provided protons of the desired energy. The proton beam was then located by searching horizontally and vertically, using the telescope coincidence counters on a rolling table which would also be displaced vertically.

Once the beam was located at two points, reasonably far apart, it was possible to set the optical axis of a cathetometer, so as to coincide exactly with the line through these two points. By the use of the cathetometer the telescope monitoring counters and the steel shield D, Fig. 2, were then aligned.

The two coincidence monitoring scintillation counters were fastened to the steel shield by special rails so that they could be removed and reinserted in the line of the beam. Each counter was marked with a dot at its center. This allowed a quick check of alignment of the counters by the cathetometer. An automatic sample holder K was also set on the axis of the beam providing a means of changing the different experimental samples with automatic alignment. The rails of the rolling table were located parallel to the proton beam in such a way that the anticoincidence counter could be dis-

placed to different distances while keeping it along the axis of the beam.

The half-angle θ subtended by the anticoincidence counter F was calculated from the distance of the center of the counter from the center of the sample.

B. Beam Collimation

The beam defined by the telescope monitor counters had very good collimation. At a distance of 12 feet it was observed that half the beam intensity remained inside a cone of only 0.3°.

The number of protons scattered out of the beam by the monitoring counters C, by the air, and by the thick walls of counter F was 1.3 percent at 10°, 2.2 percent at 3°, and 4 percent at 1°. Air attenuation makes an appreciable contribution to this effect.

C. The Adjustment and Operation of the Electronic Equipment

The electronic circuits were turned on and allowed to reach their equilibrium temperature condition. The monitoring counters C were connected in coincidence and counter F in anticoincidence. The adjustment of the electronics was carried out in the following steps. The counters C (1 and 2) were placed in the collimated proton beam and connected in double coincidence. In order to assure the time alignment of the two monitoring counters the delay of counter 1 with respect to 2 was varied; the coincidences per second were plotted as functions of the delay in millimicroseconds added to the channel of counter 2.

With the system operating on a plateau both with respect to pulse attenuation and photomultiplier voltage, the delay of counter 2 with respect to 1 was set to the value at the center of its delay curve.

Then counter F (3) was connected in anticoincidence with counters 1 and 2. The anticoincidence rate per unit of double coincidence $(1, 2, -3)/(1, 2)$ was plotted *vs* delay of counter F, for various values of voltage of the photomultiplier of F, and for various attenuations of pulse $(1, 2, -3)$ as it entered the scaler which recorded it. For the anticoincidence delay curve, a large inverted plateau curve was obtained. The delay of counter F (channel No. 3) was set to the value at the center of this delay curve. Counter F moves with the rolling table, and for each chosen distance from counters 1 and 2 the delay was adjusted to the value at the center of the corresponding new delay curve.

The shape and the width of this plateau curve gives good information about the proper operation of the over-all system including the coincidence circuit.

D. The Coulomb Scattering

The precision of the measurement of proton total nuclear cross sections depends on the accuracy of the extrapolation to zero degree angle, corresponding to the "good geometry" measurement condition. In order to obtain the best extrapolation, one must know the corrections in measurements at various angles due to Coulomb scatterings (single, plural, multiple, and the interference effect between Coulomb and diffraction scatterings).

This correction was obtained in the following way: The single Coulomb scattering correction was calculated from the Rutherford formula corrected for each special case and only this correction was applied. The remainder of the Coulomb scattering was kept to a magnitude which does not disturb the measurements and the precision of the extrapolation by a proper choice of the thickness of the target and of the angles used in the extrapolation. The multiple and plural scatterings give a large contribution only at very small angles and fall off very rapidly with increase of the subtended angle. One cannot obtain equations precise enough for corrections of these scatterings at very small angles, but by using formulas from the theory of multiple scattering it is possible to establish at which angle this scattering starts to give an appreciable contribution to the measured total cross section.

By assuming a Gaussian distribution for the multiple Coulomb scattering, and calculating the mean square deflection by the Rossi-Greisen[10] equation for the target thicknesses used in the measurement, it is found that for angles four times the mean square deflection the corresponding multiple Coulomb scattering effect is smaller than one percent of the total nuclear cross section measured.

In order to verify these results experimentally and to determine the contribution of the plural scattering and of an interference term, arising from a cross product of nuclear and Coulomb scattering, it was decided to investigate experimentally the magnitude of these Coulomb scattering effects for the worst condition; the lowest energy used, thickest target with highest Z and small angles. For that purpose the total cross section of a lead scatterer of a thickness of 7.63 g/cm^2 was measured, using protons of 214 Mev in a range of 1.4° and 15°.

From neutron cross-section data, from the measurements of Marshall, Marshall, and Nedzel,[6] and from the present measurements of total nuclear cross sections for protons on light elements one can infer the proton total cross section of lead at 214 Mev within ± 10 percent precision. At angles of the order of 1.4° the nuclear part of the total cross section is only three percent of the measured total cross section, and therefore an error of 10 percent of the nuclear cross section amounts to only 0.3 percent of the total measured cross section. Therefore, it is possible by subtraction of the nuclear cross section and single Coulomb scattering (integrated from 1.4° to 180°) from the measured total cross sections to obtain a curve corresponding

[10] B. Rossi and K. I. Greisen, Revs. Modern Phys. **13**, 240 (1941).

to the sum of the multiple plus the plural Coulomb scattering and the interference effect between Coulomb and diffraction scattering, and therefore to verify the contribution of these scatterings on the total cross section measurements.

Figure 4 shows plots of the above curves as a function of $\langle\theta^2\rangle_{Av}^{\frac{1}{2}}$. It can be seen that at four times $\langle\theta^2\rangle_{Av}^{\frac{1}{2}}$ the contribution of Coulomb scatterings is not appreciable. One can therefore safely extrapolate to zero the cross section from angles greater than $4\langle\theta^2\rangle_{Av}^{\frac{1}{2}}$. Since $\langle\theta^2\rangle_{Av}^{\frac{1}{2}}$ is a function of the square root of the thickness of absorber, one concludes that thin absorbers allow better extrapolations. However, in order to obtain good statistics with thin samples, longer cyclotron running time is needed. Hence it is necessary to compromise. It is also apparent that measurements of total cross sections of light elements provide best conditions for such extrapolations since one can use reasonably thick absorbers. With a target thickness of about 1 g/cm^2 and proper running time, it is possible to measure the cross section of elements heavier than chlorine provided appropriate corrections and careful extrapolation to "good geometry" is carried out.

The beam-monitoring coincidence counters with their light-tight shields have a thickness of about 1 g/cm^2. Therefore, by nuclear and Coulomb scattering they disturb the beam and remove about one percent of the total beam intensity at a distance of about three feet from the detector counter. During the measurements of cross section at subtended angles of about 3°, the protons have to traverse about 10 feet of air (about 0.4 g/cm^2) which also attenuates the beam. These two effects constitute part of background measurements B_0 and put a limit to the minimum thickness of sample used, since the sample extenuation should not be much smaller than the inevitable background.

E. Errors

No correction was made for charged particle production because at the energies used the total cross section for pion production is much smaller than the measured total cross section.

Since the over-all accuracy was limited by the total number of counts obtained in the attenuation measurements, because of the statistical error of counting, it was decided to have for each sample an attenuation number of counts B exceeding the normal background B_0 by at least 10 000 counts.

The beryllium attenuation at different times during the one set of measurements was observed. By this process it was verified whether drifts occur in the linearity of the equipment. When several cross sections at the same energy were to be measured, but at different running times the beryllium attenuation at 15° was observed and its consistency with the previous results within the statistical errors was assured.

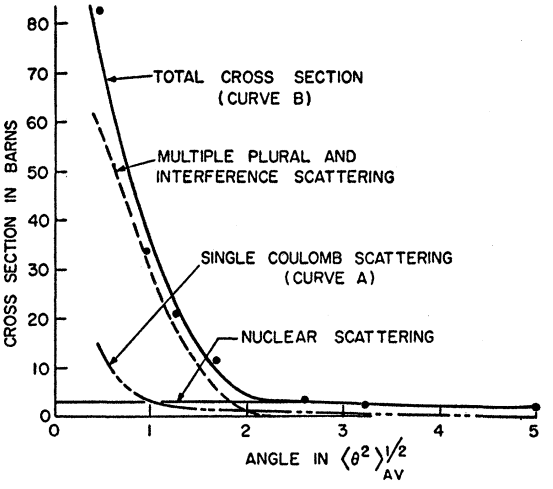

FIG. 4. The total absorption cross sections (curve B) of a lead target (with a 7.6 g/cm^2 thickness), plotted as functions of the mean square deflection produced by multiple Coulomb scattering as calculated from the Greisen-Rossi equation. (The multiple, plural, and interference scattering curve is obtained from the difference between the experimental curve B and the calculated Rutherford scattering plus the nuclear scattering curves.)

In order to detect electronic drifts the background measurement B_0 was very useful. During an experiment the background with its statistical deviation was plotted against the total number of counts and it was possible to observe abnormal deviations, if any, corresponding to drifts of the electronic circuit.

As a check against systematic errors, the cross sections were measured using the coincidence method at 315 Mev for 15°. The results by the two methods, within the statistical uncertainty, were consistent with each other. However, it is believed that experimentally the anticoincidence method is a more reliable method.

V. RESULTS

A. The Extrapolation to "Good Geometry"

To obtain the total nuclear proton cross section it is necessary to extrapolate the absorption cross section (corrected for the Rutherford scattering), measured at various angles, to zero degrees. In the range of energies used, and at the half-angle θ subtended in the measurements, most of the cross-section dependence with θ is due to the elastic scattering. The differential elastic cross section varies with the scattering angle and shows an interference pattern with a first minimum at angles which depend on the atomic mass and on the proton energy.

For energies of 208 and 315 Mev chosen for the present measurements, and for the light elements, the first-order diffraction pattern has its minimum outside of the maximum subtended angle θ and it is possible by the proper choice of a variable, such as the solid angle (in the case of the 208-Mev proton cross-section measurement), or the subtended half-angle θ (which

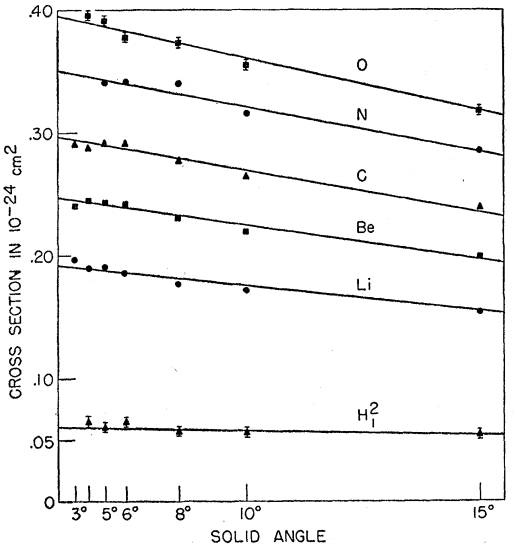

FIG. 5. Corrected cross sections for 208±4 Mev protons as a function of the laboratory-system solid angle subtended by the detector counter, showing extrapolations to zero steradians.

is more convenient for energies higher than 300 Mev) to find an almost linear relationship between the cross sections measured and the independent variable used for the extrapolation to zero degrees.

Those extrapolations are illustrated in Figs. 5 and 6.

For elements heavier than oxygen the differential cross section varies very strongly at angles much smaller than 15°, and the extrapolation loses the precision that it has for the light elements. For this reason the measurements were carried out only for elements of Z as high as chlorine, where this effect is already very pronounced. With copper, the extrapolation method used lost its precision completely.

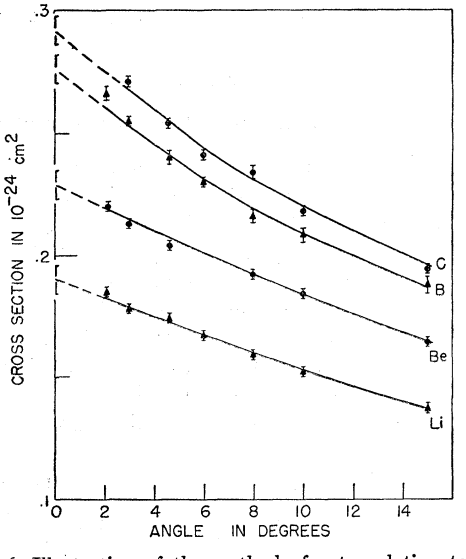

FIG. 6. Illustration of the method of extrapolation to "good geometry" used to obtain the total cross sections for 315±8 Mev protons. (The corrected cross sections measured at different geometries are plotted against the laboratory-system subtended angle θ and extrapolated to zero degrees.)

B. The Proton-Proton Scattering Cross Section

In the present work, two different methods were used to measure the total cross section of proton-proton scattering at 315±8 Mev. In the first method, following the procedure already described, the difference in the cross section in polyethylene and in graphite (with targets containing the same number of carbon atoms per square centimeter) was measured. The second method was a more precise experiment carried out with a large liquid hydrogen target. The hydrogen (with a thickness of 2.8 g/cm^2) was contained in a special Styrofoam target Dewar designed and built by

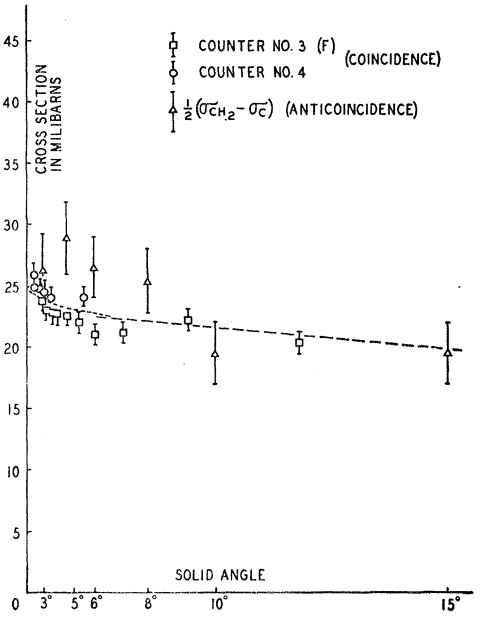

FIG. 7. Proton-proton scattering cross sections at 315±8 Mev plotted against solid angle in the laboratory system. (The dotted straight line between 6 and 15° corresponds to an average differential cross section, in the center-of-mass system, equal to 3.6 $\times 10^{-27}$ cm^2/sterad.)

Yodh[11] from a method developed at The University of Chicago by J. Marshall and L. Marshall.

At a proton energy of 208±4 Mev only the difference method (polyethylene-graphite) was used.

The cross sections obtained (corrected only for Rutherford scattering) are shown in Figs. 7 and 8. For the liquid hydrogen target the multiple Coulomb scattering correction was small even in the vicinity of two degrees, and for this reason several measurements were made at small angles in order to allow a precise extrapolation to zero degrees.

The counting system used at 315 Mev for the p-p scattering measurement in liquid hydrogen was some-

[11] G. B. Yodh (to be published).

TABLE I. Total nuclear cross sections for 315±8-Mev protons in millibarns. Corrected for single Coulomb scattering. Measured at different subtended angles θ.

Nucleus	15°	10°	8°	6°	4.65°	3°	2°	Extrapolated to 0°
Proton	20.2± 1	21.9± 1	22.4± 1	23.1± 1	23.8± 1	24.1± 1	24.2± 1	24.3± 1
Neutron	19.5± 5	26.5± 4	25.0± 4	31.8± 5	32.8± 4	26.5± 7		32.5± 4
Deuteron	39.7± 6	48.4± 5	47.4± 5	54.9± 5	56.6± 5	50.6± 8		56.8± 5
Lithium	137 ± 2	152 ± 2	159 ± 2	167 ± 2	173 ± 2	177 ± 2	185 ± 2	190 ± 6
Beryllium	164 ± 2	184 ± 2	192 ± 2	204 ± 2	213 ± 2	220 ± 2		229 ± 6
Boron	188 ± 3	208 ± 3	216 ± 4	230 ± 3	240 ± 3	255 ± 2	266 ± 3	276 ± 6
Carbon	194 ± 2	218 ± 2	234 ± 3	241 ± 2	254 ± 2	271 ± 2		292 ± 6
Nitrogen	226 ± 5	248 ± 5	267 ± 5	285 ± 5	298 ± 6	313 ± 5		340 ± 7
Oxygen	252 ± 5	277 ± 6	296 ± 6	307 ± 6	323 ± 6	350 ± 6		379 ±10
Aluminum	358 ± 6	402 ± 8	435 ± 8	472 ± 8	508 ± 9	553 ±11		580 ±16
Sulfur	408 ± 8	458 ± 9	494 ± 9	540 ±10	580 ±10	624 ±15		686 ±18
Chlorine	438 ±10	493 ±10	532 ±10	590 ±11	630 ±11	678 ±18		749 ±20

what different from that used in other measurements. Instead of the anticoincidence method, the coincidence method was used and not only one, but two counters, one behind the other on the axis of the beam, were used as detector counters for the measurement of the ratio (I_0/I). With this arrangement it was possible to measure simultaneously the cross sections corresponding to two different subtended angles θ, with economy of running time. I_0 was obtained with the Styrofoam target placed in the beam but no liquid hydrogen in it, and I was obtained with the hydrogen in.

Since the ratio of solid angle in the laboratory system to solid angle in the center-of-mass system, $(d\Omega/d\omega)_\theta$, does not vary much in the range of angles used, one can assume for it an average value. Between 6° and 15° this average value of $(d\Omega/d\omega)_\theta$ is about 0.231. It is possible to fit a straight line to the p-p scattering measurements, which is consistent with a slope corresponding to a $\langle d\sigma/d\omega\rangle_{Av}$ equal to 3.6×10^{-27} cm²/sterad. However, at angles smaller than 6° the differential cross section seems to increase. The slope of the straight line fitted to 208-Mev data corresponds to an average value of $\langle d\sigma/d\omega\rangle_{Av}$ equal to 3.4×10^{-27} cm²/sterad between 6° and 15° (see Figs. 7 and 8).

Within the experimental error the total cross sections of p-p scattering obtained in the present experiments do not vary with energy and are in good agreement with

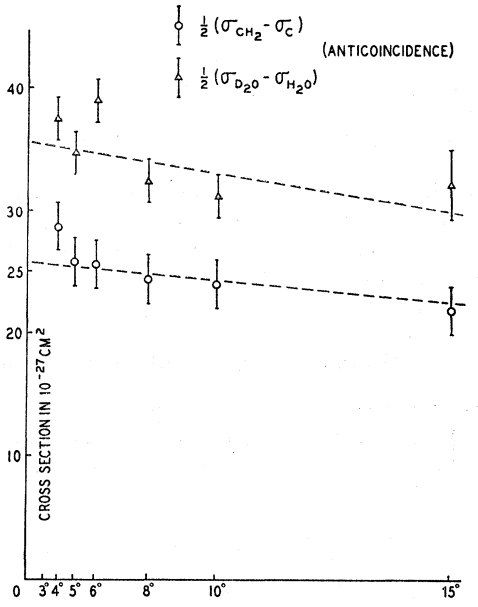

FIG. 8. Proton-proton scattering cross sections at 208±4 Mev plotted against solid angle in the laboratory system. Lower curve, proton-proton; upper curve, proton-neutron. (The dotted straight line fitting the experimental proton-proton values is consistent with an average value of 3.4×10^{-27} cm²/sterad for the differential cross section in the center-of-mass system.)

TABLE II. Total nuclear cross sections for 208±4-Mev protons in millibarns. Corrected for single Coulomb scattering. Measured at different subtended angles θ.

Nucleus	15°	10°	8°	7°	6°	5°	4°	3°	Extrapolated to 0°
Proton	22.0±2	24.0±2	24.4±2		25.6±2	25.8±2	28.7±2		25.8± 2.0
Neutron	32.2±3	31.2±2	32.4±2		39.0±2	34.7±2	36.5±2		37.0± 2.0
Deuteron	54.2±5	55.2±4	56.8±4		64.8±4	60.5±4	65.2±4		62.8± 3.0
Lithium	153 ±1	172 ±1	177 ±1		186 ±1	191 ±1	189 ±1	197±1	192 ± 3
Beryllium	198 ±1	219 ±1	231 ±1		242 ±2	243 ±2	245 ±1	240±2	247 ± 6
Boron	206 ±3	232 ±3	245 ±2	260±3	253 ±3	272 ±3	270 ±3	275±3	276 ± 9
Carbon	238 ±1	264 ±1	277 ±1		291 ±1	291 ±1	287 ±1	290±2	296 ± 3
Nitrogen	285 ±1	314 ±3	330 ±2		341 ±2	341 ±2			350 ±10
Oxygen	320 ±7	355 ±6	373 ±6		378 ±6	392 ±6	396 ±6		395 ±10
Aluminum	467 ±4	485 ±3	506 ±3		528 ±3	556 ±2	588 ±3		592 ±10
Sulfur	494 ±4	530 ±7	560 ±9		591 ±8	608 ±9	666 ±7		680 ±20
Chlorine	515 ±3	563 ±6	571 ±6		619 ±6	659 ±7	687 ±4		740 ±20

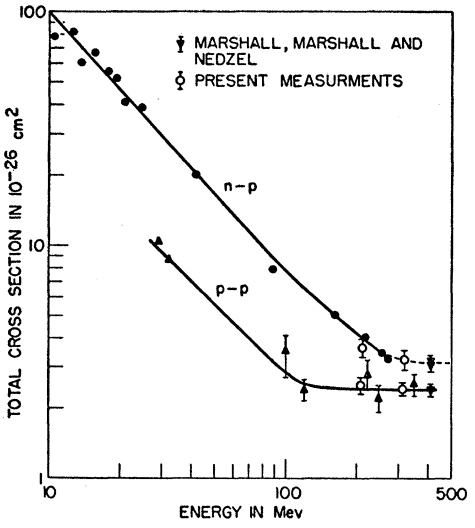

FIG. 9. Total cross sections for n-p scattering, σ_{np}, and p-p scattering, σ_{pp}, at various energies from the available published values. (The results obtained in this study are also included.)

the results of previous measurements.[12,13] The total nuclear cross sections of 315 and 208 Mev protons in millibarns corrected for single Coulomb scattering and measured at different subtended angles θ are shown in Tables I and II.

C. The Proton-Neutral Total Cross Section

Measurements of the scattering of protons by neutrons were carried out using D_2O and H_2O measured in the same geometry and with the same number of molecules per cm². The neutron cross sections were then $\frac{1}{2}[\sigma(D_2O)-\sigma(H_2O)]$.

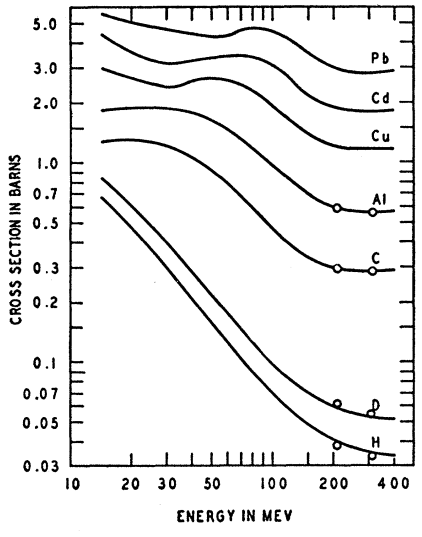

FIG. 10. Total neutron cross sections as a function of energy as compared with the proton cross sections measured at the same energies.

In Fig. 9 the results are compared with the previous work done at different energies.[14–20] One can observe that for energies lower than 100 Mev, σ_{np} has a $1/E$ dependence. At energies higher than 100 Mev the energy dependence appears to vary somewhat more slowly than $1/E$, and from the result of the present measurement it seems that the cross sections tend to be energy-independent for energies higher than 300 Mev.

D. Comparison with Neutron Cross Sections

From a compilation by Nedzel[2] of the available neutron cross sections it was possible to draw smooth curves fitting the experimental data, showing how the neutron cross section varies with the neutron energy. The proton cross sections are compared with those neutron cross sections at the same energy in Fig. 10 and in Table III.[2,6,20,21]

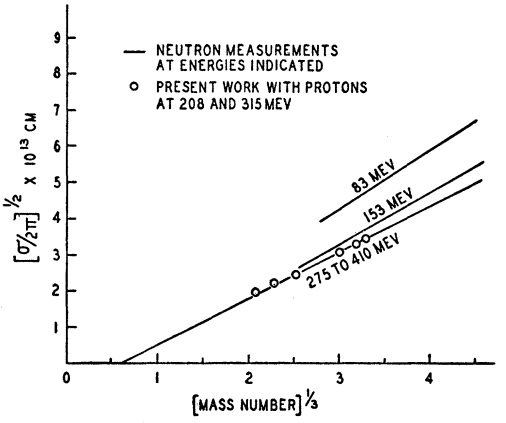

FIG. 11. The effective nuclear radii for nucleons $(\sigma/2\pi)^{\frac{1}{2}}$ plotted as functions of $A^{\frac{1}{3}}$. (For neutrons of the energies indicated and for protons at 208 Mev and 315 Mev, for comparison. The negative intercept is clearly shown.)

The comparison shows evidence for support of the charge symmetry hypothesis.

From the results of measurement of the total cross section for fast neutrons the nuclear radius is expressed by the equation

$$R=a+r_0A^{\frac{1}{3}}, \qquad (3)$$

which is consistent with the hypothesis of constant density of the nuclear matter. A positive intercept may be related to range of nuclear forces. If this range is

[12] Chamberlain, Pettengill, Segrè, and Wiegand, Phys. Rev. **93**, 1424 (1954).
[13] Marshall, Marshall, and Nedzel, Phys. Rev. **85**, 416 (1952).
[14] W. Sleator, Phys. Rev. **72**, 207 (1947).
[15] R. Sherr, Phys. Rev. **68**, 240 (1945).
[16] R. H. Hildebrand and C. E. Leith, Phys. Rev. **80**, 842 (1950).
[17] Hadley, Kelly, Leith, Segrè, Wiegand, and York, Phys. Rev. **75**, 351 (1949).
[18] Kelly, Leith, Segrè, and Wiegand, Phys. Rev. **79**, 96 (1950).
[19] J. De Juren and B. J. Moyer, Phys. Rev. **81**, 919 (1951).
[20] Fox, Leith, Wouters, and MacKenzie, Phys. Rev. **80**, 23 (1950).
[21] J. De Juren and N. Knable, Phys. Rev. **80**, 27 (1950).

TABLE III. A summary of high-energy neutron and proton cross sections in millibarns. The first three columns show the published neutron cross sections for 410 Mev,[a] 280 Mev,[b] and 270 Mev.[c] The fourth column shows published value for 408-Mev[d] protons, and in the fifth and sixth columns the results of present work are given for 208-Mev and 315-Mev protons.

	Neutrons			Protons		
	410 Mev	280 Mev	270 Mev	408 Mev	315 Mev	208 Mev
H	33.7±1.3	33± 3	38±1.5	31.6±2	32.5± 4	36.5± 4
D	62 ±4	49± 5	57±3	55.6±3	56.8± 5	61.0± 4
Be	231 ±4	225± 4	229±3	242 ±6	229 ± 6	247 ± 4
C	297 ±3	279± 4	288±3	285 ±4	292 ± 6	296 ± 4
O	278 ±5	380± 8	372±7	406 ±3	379 ±10	395 ± 8
Al	587 ±7	566±18	555±8		580 ±16	592 ±10
S	672 ±9				686 ±18	680 ±20
Cl	742 ±9				740 ±20	740 ±20

[a] See reference 2.
[b] See reference 20.
[c] See reference 21.
[d] See reference 6.

a very short one the equation may be written as

$$R=r_0A^{\frac{1}{3}}. \tag{4}$$

A negative value for the intercept has no physical meaning if one assumes an opaque sphere model of the nucleus and a constant density of nuclear matter.

It was found in the present investigation that the radii R obtained from the measured cross sections (using the opaque sphere model) when plotted against $A^{\frac{1}{3}}$, show a negative intercept (see Fig. 11), and also that the slope of the straight line fitting the experimental data is consistent with a nuclear radius

$$R=-0.4+1.19\times A^{\frac{1}{3}}, \tag{5}$$

in units 10^{-13} cm, which may be considered as too small.

These results can be explained by a partial nuclear transparency to the high energy protons. The actual radius can be obtained from the optical model of Fernbach, Serber, and Taylor.

This model predicts a total cross section (when the refractive index of the nuclear matter is one) given by an equation depending only on K (absorption coefficient) and the nucleon radius R,

$$\sigma_t=2\pi R^2\left\{1-2\left[\frac{1-(1+KR)\exp(-KR)}{K^2R^2}\right]\right\}. \tag{6}$$

The best fit for the proton cross-section measurement to this equation corresponds to $R=1.23\times10^{-13}$ cm and $K=0.5\times10^{13}$ cm^{-1}. These are the same as the values calculated by Nedzel[2] for neutrons.

VI. ACKNOWLEDGMENTS

The author wishes to express his appreciation to Professor Herbert L. Anderson, from the Institute for Nuclear Studies of The University of Chicago, for his encouragement and for the author's appointment as a Research Associate in the Institute, to Professor John Marshall for his guidance, help and encouragement, to Dr. L. Marshall for valuable suggestions, to Mr. J. Fischer for assistance with the electronics and to the cyclotron staff, particularly to Mr. Lester Kornblith, Jr., for helpful cooperation.

The author wishes to express his appreciation to Mr. M. D. A. Anastacio, M. Campos, and E. Heiberg for help during the experiments.